

# Area laws and thermalization from classical entropies in a Bose-Einstein condensate

Yannick Deller,<sup>1</sup> Martin Gärttner,<sup>2</sup> Tobias Haas,<sup>3,\*</sup> Markus K. Oberthaler,<sup>1</sup> Moritz Reh,<sup>1,2</sup> and Helmut Strobel<sup>1</sup>

<sup>1</sup>*Kirchhoff-Institut für Physik, Universität Heidelberg,  
Im Neuenheimer Feld 227, 69120 Heidelberg, Germany*

<sup>2</sup>*Institut für Festkörperteorie und Optik, Friedrich-Schiller-Universität Jena, Max-Wien-Platz 1, 07743 Jena, Germany*

<sup>3</sup>*Centre for Quantum Information and Communication, École polytechnique de Bruxelles,  
CP 165, Université libre de Bruxelles, 1050 Brussels, Belgium*

The scaling of local quantum entropies is of utmost interest for characterizing quantum fields, many-body systems, and gravity. Despite their importance, theoretically and experimentally accessing quantum entropies is challenging as they are nonlinear functionals of the underlying quantum state. Here, we show that suitably chosen classical entropies capture the very same features as their quantum analogs for an experimentally relevant setting. We describe the post-quench dynamics of a multi-well spin-1 Bose-Einstein condensate from an initial product state via measurement distributions of spin observables and estimate the corresponding entropies using the asymptotically unbiased  $k$ -nearest neighbor method. We observe the dynamical build-up of quantum correlations signaled by an area law, as well as local thermalization revealed by a transition to a volume law, both in regimes characterized by non-Gaussian distributions. We emphasize that all relevant features can be observed at small sample numbers without assuming a specific functional form of the distributions, rendering our method directly applicable to a large variety of models and experimental platforms.

*Introduction* — The quantum entropy of a spatial subregion has proven to serve as a ubiquitous tool for studying the spatio-temporal structure of entanglement [1] and its role in various quantum phenomena, including local thermalization [2–5], quantum phase transitions [6], information scrambling [7–9] and black hole physics [10–13]. Arguably the most sought-after phenomenon in this context is the area law, which is signaled by a logarithmic growth of the local entropy for one-dimensional systems [14–22]. It appears at short times after quenching the couplings of a locally interacting system, that was initially prepared in a product state – a scenario that can be readily realized experimentally [22]. At later times the system typically thermalizes and the local entropy instead obeys a volume law, allowing for a macroscopic description using only a few thermodynamic quantities like temperature.

The main drawback of quantum entropic descriptions for many-body phenomena is their reliance on the knowledge of the full density matrix, which grows exponentially with the number of microscopic constituents. This has so far restricted the experimental access of quantum entropies to systems consisting of a few particles [23–25], as full tomography of the quantum state is, with no further assumptions, infeasible for larger systems approaching mesoscopic scales. For continuous systems, area laws have only been experimentally reported in a Gaussian scenario [26], while generally applicable methods have remained elusive.

Recently, the necessity of considering exclusively *quantum* entropies to probe quantum phenomena has been questioned. Suitably chosen *classical* entropies of (quasi-)probability distributions also encode area and volume laws [27]. This insight naturally overcomes the need for reconstructing the full quantum state – both for theoretic-

cal and experimental investigations. Thus the observation of entropic scaling behavior becomes accessible for experimental platforms, which can directly sample from such distributions, see for example [28–36].

Here we show that area and volume laws are observable in state-of-the-art experiments with multi-well spin-1 Bose-Einstein condensates (BECs) [37, 38] by considering entropies of measurement distributions over spin observables. Starting from an initial product state, we find area laws being dynamically generated for intermediate evolution times following a quench, thereby confirming the growth of entanglement until the system thermalizes locally, where the same entropies exhibit volume law behavior. Importantly, we do so without making assumptions about the functional form of the state and only rely on observables that are directly obtainable in standard experimental readouts [26, 31, 34–36], while reducing the sample complexity to a feasible level. We comprehensively discuss our method, including systematic checks for its validity and generality, in [39].

*Notation* — We use natural units  $\hbar = k_B = 1$ , write bold (normal) letters for quantum operators  $\mathbf{O}$  (classical variables  $O$ ) as well as their traces and equip vacuum expressions with a overbar, e.g.  $\bar{\rho}$ .

*Multi-Well Spin-1 BEC* — We consider a one-dimensional lattice of spin-1 BECs that extends over 20 wells, described by bosonic mode operators  $[\mathbf{a}_{m_F}^j, \mathbf{a}_{m'_F}^{j'\dagger}] = \delta^{jj'} \delta_{m_F m'_F}$  with  $j \in \{1, \dots, N\}$  and  $m_F \in \{0, \pm 1\}$ . Starting from an initial product state with all zero modes ( $m_F = 0$ ) being occupied coherently with a mean number of  $n = 10^3$  atoms, we consider the evolution under the

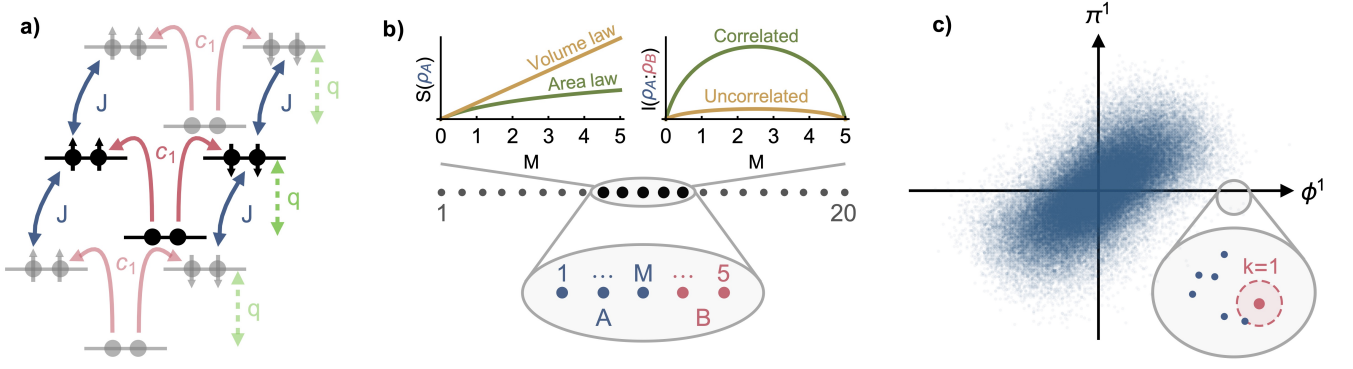


Figure 1. **a)** Illustration of relevant processes. The  $\pm 1$  modes of a spin-1 BEC are coupled to the 0 mode by spin-changing collisions with strength  $c_1 < 0$  (red) and detuned by the quadratic Zeeman-shift  $q > 0$  (green). The atoms in the  $\pm 1$  modes may hop to neighboring wells with strength  $J > 0$  (blue). **b)** The full system consists of 20 wells, from which we exclusively analyze the five wells 8 – 12. We partition this subsystem into a left part  $A$  (blue) and a right part  $B$  (red) and study the scalings of information and correlation measures with  $A$ 's system size  $M$ . **c)** Samples of the Wigner  $W$ -distribution of the left-most well in subsystem  $A$  at time  $t = 4$ . The entropy is estimated from samples using the  $k$ NN-estimator by analyzing the distribution of distances to the  $k$ -th. neighbor for each sample, see magnified inset. Non-Gaussian features arise for higher-dimensional multi-well distributions, as measured by the relative entropy, see [40].

Hamiltonian

$$\begin{aligned}
 H = & \sum_{j=1}^{20} q \left( N_1^j + N_{-1}^j \right) + c_0 N^j (N^j - 1) \\
 & + c_1 \left[ \left( N_0^j - (1/2)\mathbb{1} \right) \left( N_1^j + N_{-1}^j \right) \right. \\
 & \quad \left. + a_0^{j\dagger} a_0^j a_1^j a_{-1}^j + a_1^{j\dagger} a_{-1}^j a_0^j a_0^j \right] \\
 & - J \sum_{j=1}^{19} \sum_{m_F=\pm 1} \left( a_{m_F}^{j\dagger} a_{m_F}^{j+1} + a_{m_F}^{(j+1)\dagger} a_{m_F}^j \right),
 \end{aligned} \tag{1}$$

featuring dynamics within single wells (first sum) as well as correlation build-up among wells (second sum), see Figure 1 a).

For early times, the zero mode is occupied macroscopically and the evolution is dominated by second-order fluctuations, such that (1) is well-approximated by an analytically solvable Gaussian model, which follows from treating the zero mode classically and dropping density-density interactions (see [39] for details)

$$\begin{aligned}
 H_{\text{up,Gauss}} = & \sum_{j=1}^{20} \left[ \tilde{q} N^j + \frac{\tilde{c}_1}{2} \left( \mathbf{a}^j \mathbf{a}^j + \mathbf{a}^{j\dagger} \mathbf{a}^{j\dagger} \right) \right] \\
 & - J \sum_{j=1}^{19} \left( \mathbf{a}^{j\dagger} \mathbf{a}^{j+1} + \mathbf{a}^{(j+1)\dagger} \mathbf{a}^j \right).
 \end{aligned} \tag{2}$$

Here, we introduced the relative mode operators  $\mathbf{a}^j = (\mathbf{a}_1^j + \mathbf{a}_{-1}^j)/\sqrt{2}$  as well as the rescaled couplings  $\tilde{c}_1 = c_1 n$  and  $\tilde{q} = c_1 \left( n - \frac{1}{2} \right) + q$ .

Beyond this regime, the high occupation justifies employing semi-classical approaches such as the truncated Wigner approximation (TWA), in which the mode operators are demoted to  $c$ -numbers that obey an evolution

dictated by classical mean field equations [41, 42]. The resulting model correctly captures the quantum fluctuations of the initial state, while neglecting higher-order corrections in  $\hbar$  for its evolution.

*Measurement distributions* — We analyze the information content of a subsystem of five wells (see Figure 1 b)) in terms of measurement distributions using phase-space methods. We focus on the two normalized spin-1 observables [37, 38]

$$\begin{aligned}
 \phi^j & \equiv \frac{S_x^j}{\sqrt{2n}} = \frac{1}{\sqrt{2}} \left[ a_0^{j\dagger} \left( a_1^j + a_{-1}^j \right) + h.c. \right] / \sqrt{2n}, \\
 \pi^j & \equiv -\frac{Q_{yz}^j}{\sqrt{2n}} = \frac{-i}{\sqrt{2}} \left[ a_0^{j\dagger} \left( a_1^j - a_{-1}^j \right) - h.c. \right] / \sqrt{2n},
 \end{aligned} \tag{3}$$

which form a set of pairwise canonically conjugate operators  $[\phi^j, \pi^{j'}] = i\delta^{jj'} \mathbb{1}$  with corresponding bosonic mode operators  $\mathbf{a}^j, \mathbf{a}^{j\dagger}$  in the early-time regime [39]. Their Wigner  $W$ -distribution is defined via [43]

$$\begin{aligned}
 \mathcal{W}^j & \equiv \mathcal{W}^j(\phi^j, \pi^j) \\
 & = \int \frac{d\tilde{\phi}^j d\tilde{\pi}^j}{2\pi} e^{-i(\phi^j, \pi^j)\Omega(\tilde{\phi}^j, \tilde{\pi}^j)^T} \\
 & \quad \times \text{Tr} \left\{ \rho^j e^{i(\phi^j, \pi^j)\Omega(\tilde{\phi}^j, \tilde{\pi}^j)^T} \right\},
 \end{aligned} \tag{4}$$

with the symplectic form  $\Omega = i\sigma_2$  and  $\sigma_2$  being the second Pauli matrix. As  $\mathcal{W}^j$  is only accessible through costly Wigner tomography [44, 45], it is mainly of theoretical interest. Let us therefore also introduce more experimentally convenient distributions, namely the Wigner marginals  $f^j \equiv f^j(\phi^j) = \int d\pi^j \mathcal{W}^j$  and  $g^j \equiv g^j(\pi^j) = \int d\phi^j \mathcal{W}^j$ , accessible through homodyne measurements [28], as well as the Husimi  $Q$ -distribution, which is obtained by projecting onto the coherent states

$|\alpha^j\rangle = \exp(\alpha^j \mathbf{a}^{j\dagger} - \alpha^{j*} \mathbf{a}^j) |0^j\rangle$  [31, 34–36, 46], with  $\alpha^j = (\phi^j + i\pi^j)/\sqrt{2}$ , leading to [47, 48]

$$\mathcal{Q}^j \equiv \mathcal{Q}^j(\phi^j, \pi^j) = \mathbf{Tr} \{ \rho^j |\alpha^j\rangle \langle \alpha^j| \}. \quad (5)$$

*Information and correlations from classical distributions* — To analyze the local information content of the subsystem, we consider differential entropies of the classical distributions  $\mathcal{O}^A$  with respect to its left part  $A$  (see Figure 1 b))

$$S(\mathcal{O}^A) = - \int d\nu^A \mathcal{O}^A \ln \mathcal{O}^A, \quad (6)$$

where the integral measure  $d\nu^A$  depends on the distribution under scrutiny [49]. We note that (6) is always well-defined for the non-negative marginal and Husimi  $Q$ -distributions, but is restricted to Wigner-positive states when applied to  $\mathcal{W}^A$ , which is an assumption implicitly made when working within TWA or Gaussian models.

Being measures of disorder, classical entropies over incompatible observables are bounded from below by their vacuum values via entropic uncertainty relations [50–55] (see [56, 57] for reviews). When considered for quantum many-body systems, these bounds scale with the number of modes, i.e.  $S(\bar{\mathcal{O}}^A) \sim M$ , showing that classical entropies are extensive to leading order as a result of vacuum contributions [58, 59]. However, as shown in [27], scalings induced by quantum phenomena, such as the area law, manifest themselves in the *next-to-leading* order terms. Thus, we define the so-called subtracted classical entropies as [27]

$$\Delta S(\mathcal{O}^A) \equiv S(\mathcal{O}^A) - S(\bar{\mathcal{O}}^A), \quad (7)$$

with the extensive vacuum contribution  $S(\bar{\mathcal{O}}^A) \sim M$  being subtracted [60].

Let us further consider the classical version of the archetypical measure for correlations between the left and right parts of the subsystem, that is, the classical mutual information

$$I(\mathcal{O}^A : \mathcal{O}^B) = S(\mathcal{O}^A) + S(\mathcal{O}^B) - S(\mathcal{O}). \quad (8)$$

Being already defined via a relative entropic measure, no vacuum contributions have to be subtracted to reveal quantum features.

*Connections to quantum information theory* — In the context of the Gaussian model (2), the connection between subtracted classical and quantum entropies becomes a simple equality: in this case, we can establish  $\Delta S(\mathcal{W}^A) = S_2(\rho^A)$ , where  $S_2(\rho^A)$  denotes the Rényi-2 entropy of the density matrix associated to  $\mathcal{W}^A$  [61]. Beyond Gaussianity, such simple relations can only be established for the subtracted Rényi-2 entropy of  $\mathcal{W}^A$  [62]. However, in the following, we provide strong evidence that the scaling of the subtracted classical entropies (7) also extends to the non-Gaussian interacting case.

Furthermore, a connection to the quantum mutual information in the case of Gaussian states is straightforward and reads  $I(\mathcal{W}^A : \mathcal{W}^B) = I_2(\rho^A : \rho^B)$  [61]. More generally, classical mutual informations constitute lower bounds to their quantum analogs by the uncertainty principle, i.e. [54, 63]

$$I(\mathcal{O}^A : \mathcal{O}^B) \leq I(\rho^A : \rho^B), \quad (9)$$

which are expected to be tighter than second-moment bounds beyond Gaussian states [64]. An immediate consequence of (9) is that the standard argument for the appearance of the area law for local interactions and thermal states presented in [65] applies also to any classical mutual information [27]. Hence, classical mutual information, albeit typically not capturing all quantum correlations, shows the finite-size area law whenever its quantum analog does.

*Methods* — We generate  $10^4$  synthetic samples for the three distributions of our interest using TWA to simulate an experiment showcasing the feasibility of the proposed approach. In contrast to the estimation of low-order moments, extracting entropic quantities from a set of samples is more involved, since they are *functionals* of the underlying distributions. Given a set of samples, we employ the established  $k$ -nearest neighbor ( $k$ NN) method devised in [66–68] using information about the statistics of the nearest neighbors of each sample (see Figure 1 c)), to arrive at an estimate of its local density. These results are validated against the analytically solvable model (2) in the early-time regime. We give a more comprehensive validation of the  $k$ NN-estimator for our setup in [39]. Further, we define an energy scale by setting  $nc_1 = -1$ , consider Lithium-7 with  $c_0 = -2c_1$  and set the quench parameters to  $q = 4, J = 2$ , for which non-Gaussian features arise around  $t = 3$ .

While the total system undergoes a unitary evolution dictated by the Hamiltonian in Eq. (1), the considered subsystem does not, as its entanglement with the rest of the system implies a mixed reduced density matrix [69]. In the following, we demonstrate the area law and local thermalization for the theoretically interesting, but experimentally difficult to access subtracted Wigner entropy, as well as for the experimentally amenable subtracted marginal entropy sum  $\Delta S(f^A) + \Delta S(g^A)$ , and the so-called Wehrl mutual information  $I(\mathcal{Q}^A : \mathcal{Q}^B)$  (additional quantities are discussed in [40]).

*Area law* — We first study the early-time regime, that is,  $t \leq 4$ , in the upper row of Figure 2. At  $t = 0$ , the subsystem is in a pure product state, and all entropic measures evaluate to zero. Around  $t = 1$ , correlations among the wells start to build up, causing subsystem  $A$  to become entangled with its complement  $B$ . In this regime, subtracted classical entropies obey the area law, i.e. a logarithmic growth with system size  $M$ ,

$$\Delta S(\mathcal{O}^A) = \kappa_1 \ln(M + \kappa_2) + \kappa_3, \quad (10)$$

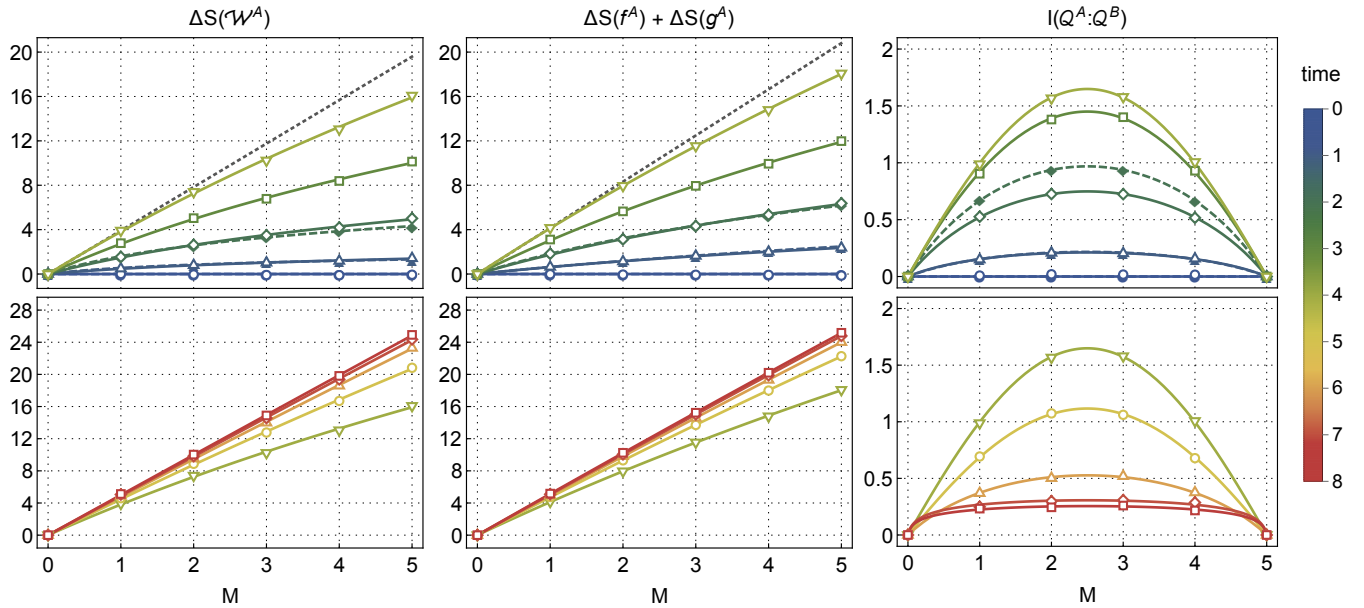


Figure 2. Analysis regarding the presence of area and volume laws at early times  $t = 0, 1, 2, 3, 4$  (upper row) and late times  $t = 4, 5, 6, 7, 8$  (lower row), respectively. Open (closed) plot markers denote TWA (analytic) results and the corresponding solid (dashed) curves are fits. In the early-time regime, we observe the subtracted classical entropies to fulfill a logarithmic growth with subsystem size in the sense of (10) (see [40] for the *standard* Wigner entropy). Their sublinear scaling is highlighted for  $t = 4$  by straight lines (gray dotted), which are fitted to the first two data points. In accordance, we also find the finite-size area law (11) for the Wehrl mutual information. These findings hold true for both the TWA and the analytical approach, which agree in the Gaussian regime, i.e. up to  $t = 3$  [40], thereby also validating the  $k$ NN estimator. For later times, the area law of the subtracted classical entropies tends into a stationary volume law (12), thereby demonstrating local thermalization. After the stationary point  $t = 7$ , the local temperature can be extracted via their inclines, which consistently yields  $T \approx 5$ . The appearance of local thermalization is further supported by the decreasing correlations between  $A$  and  $B$  towards zero as revealed by the evolution of the Wehrl mutual information.

just as one would expect for the entanglement entropy [14–22]. The fit parameters  $\kappa_i$  are constrained by  $\kappa_2 = e^{-\kappa_3/\kappa_1}$  to ensure  $\Delta S(\mathcal{O}^A) = 0$  when  $M = 0$ . Around  $t = 3$ , the distributions begin to exhibit non-Gaussian features, which we quantify by the relative entropy with respect to the closest Gaussian distribution, see [40].

Similarly, the Wehrl mutual information signals the generation of correlations between  $A$  and  $B$  in terms of the finite-size area law [14]

$$I(\mathcal{O}^A : \mathcal{O}^B) = \kappa_1 \ln \left[ \frac{5}{\pi} \sin \left( \frac{\pi M}{5} \right) + \kappa_2 \right] + \kappa_3, \quad (11)$$

which incorporates the reflection symmetry around  $M = 2.5$ . Again, the behavior coincides with what is expected for the quantum mutual information [65], with maximal correlations occurring at  $t = 4$ .

*Local thermalization* — For later times, i.e. in the regime  $t \geq 4$  (lower row of Figure 2), the subtracted classical entropies transition from an intermediate stage around  $t = 5$  to an extensive growth with system size at  $t = 7$ . The latter remains stationary beyond  $t = 7$ , signaling that the system has thermalized locally in the considered degrees of freedom, with the remaining system serving as a heat bath. In this case, all entropies of our

interest obey the volume law [3]

$$\Delta S(\mathcal{O}^A) = \beta M, \quad (12)$$

where  $\beta = 1/T$  denotes the inverse local temperature. Indeed, both final entropic curves show an incline of  $T \approx 5$ , illustrating how the local temperature can be extracted from classical entropies by simple means. We have checked that this temperature depends only weakly on the quench parameters, as the dominating energy scale is set by the fourth-order term proportional to  $c_0$  in (1).

While the classical entropies become extensive, the Wehrl mutual information still obeys the finite-size area law (11) for later times, which also highlights its robustness against thermal fluctuations. In contrast to the early-time dynamics, the correlations between  $A$  and  $B$  now decline monotonically towards local thermal equilibrium.

*Discussion* — We have demonstrated that quantum many-body phenomena can be probed with classical entropies by considering a concrete model system that can be readily realized experimentally. Specifically, we have shown that it is possible to observe the area law, that is, the characteristic logarithmic growth of the entanglement entropy, and the volume law, which indicates local thermalization, via subtracted classical entropies and mutual

informations of experimentally accessible measurement distributions. Crucially, we have not assumed the state to obey a specific functional form and only relied on  $10^4$  samples which we deem experimentally feasible. Future work will address what other parallels between classical entropies and quantum entropies exist, especially for other degrees of freedom, and whether they also lend themselves as easily to experimental implementations as in the discussed work.

*Acknowledgements* — The authors thank Thomas Gasenzer and Ido Siovitz for helpful discussions during the development of the manuscript. T. H. is supported by the European Union under project ShoQC within the ERA-NET Cofund in Quantum Technologies (QuantERA) program, as well as by the F.R.S.- FNRS under project CHEQS within the Excellence of Science (EOS) program. This work is supported by the Deutsche Forschungsgemeinschaft (DFG, German Research Foundation) under Germany’s Excellence Strategy EXC2181/1-390900948 (the Heidelberg STRUCTURES Excellence Cluster) and within the Collaborative Research Center SFB1225 (ISO-QUANT). This work was partially financed by the Baden-Württemberg Stiftung gGmbH. The authors gratefully acknowledge the Gauss Centre for Supercomputing e.V. (www.gauss-centre.eu) for funding this project by providing computing time through the John von Neumann Institute for Computing (NIC) on the GCS Supercomputer JUWELS [70] at Jülich Supercomputing Centre (JSC).

---

\* tobias.haas@ulb.be

- [1] R. Horodecki, P. Horodecki, M. Horodecki, and K. Horodecki, Quantum entanglement, *Rev. Mod. Phys.* **81**, 865 (2009).
- [2] S. Popescu, A. Short, and A. Winter, Entanglement and the foundations of statistical mechanics, *Nat. Phys.* **2**, 754 (2006).
- [3] D. A. Abanin, E. Altman, I. Bloch, and M. Serbyn, Colloquium: Many-body localization, thermalization, and entanglement, *Rev. Mod. Phys.* **91**, 021001 (2019).
- [4] N. Dowling, S. Floerchinger, and T. Haas, Second law of thermodynamics for relativistic fluids formulated with relative entropy, *Phys. Rev. D* **102**, 105002 (2020).
- [5] S. Floerchinger and T. Haas, Thermodynamics from relative entropy, *Phys. Rev. E* **102**, 052117 (2020).
- [6] T. J. Osborne and M. A. Nielsen, Entanglement in a simple quantum phase transition, *Phys. Rev. A* **66**, 032110 (2002).
- [7] R. Jozsa and N. Linden, On the Role of Entanglement in Quantum-Computational Speed-Up, *Proc. Math. Phys. Eng. Sci.* **459**, 2011 (2003).
- [8] K. A. Landsman, C. Figgatt, T. Schuster, N. M. Linke, B. Yoshida, N. Y. Yao, and C. Monroe, Verified quantum information scrambling, *Nature* **567**, 61 (2019).
- [9] S. Xu and B. Swingle, Scrambling Dynamics and Out-of-Time-Ordered Correlators in Quantum Many-Body Systems, *PRX Quantum* **5**, 010201 (2024).
- [10] L. Bombelli, R. K. Koul, J. Lee, and R. D. Sorkin, Quantum source of entropy for black holes, *Phys. Rev. D* **34**, 373 (1986).
- [11] M. Srednicki, Entropy and area, *Phys. Rev. Lett.* **71**, 666 (1993).
- [12] C. Callan and F. Wilczek, On geometric entropy, *Phys. Lett. B* **333**, 55 (1994).
- [13] S. N. Solodukhin, Entanglement Entropy of Black Holes, *Living Rev. Relativ.* **14**, 8 (2011).
- [14] P. Calabrese and J. Cardy, Entanglement entropy and quantum field theory, *J. Stat. Mech. Theo. Exp.* **2004**, P06002 (2004).
- [15] P. Calabrese and J. Cardy, Entanglement Entropy and Quantum Field Theory: A Non-Technical Introduction, *Int. J. Quantum Inf.* **04**, 429 (2006).
- [16] M. B. Plenio and S. Virmani, An Introduction to Entanglement Measures, *Quantum Inf. Comput.* **7**, 1–51 (2007).
- [17] M. B. Hastings, An area law for one-dimensional quantum systems, *J. Stat. Mech.: Theo. Exp.* **2007**, P08024 (2007).
- [18] L. Amico, R. Fazio, A. Osterloh, and V. Vedral, Entanglement in many-body systems, *Rev. Mod. Phys.* **80**, 517 (2008).
- [19] P. Calabrese and J. Cardy, Entanglement entropy and conformal field theory, *J. Phys. A Math. Theo.* **42**, 504005 (2009).
- [20] H. Casini and M. Huerta, Entanglement entropy in free quantum field theory, *J. Phys. A Math. Theo.* **42**, 504007 (2009).
- [21] I. Peschel and V. Eisler, Reduced density matrices and entanglement entropy in free lattice models, *J. Phys. A: Math. Theo.* **42**, 504003 (2009).
- [22] J. Eisert, M. Cramer, and M. B. Plenio, Colloquium: Area laws for the entanglement entropy, *Rev. Mod. Phys.* **82**, 277 (2010).
- [23] R. Islam, R. Ma, P. M. Preiss, M. E. Tai, A. Lukinand, M. Rispoli, and M. Greiner, Measuring entanglement entropy in a quantum many-body system, *Nature* **528**, 77 (2015).
- [24] A. M. Kaufman, M. E. Tai, A. Lukin, M. Rispoli, R. Schittko, P. M. Preiss, and M. Greiner, Quantum thermalization through entanglement in an isolated many-body system, *Science* **353**, 794 (2016).
- [25] T. Brydges, A. Elben, P. Jurcevic, B. Vermersch, C. Maier, B. P. Lanyon, P. Zoller, R. Blatt, and C. F. Roos, Probing Rényi entanglement entropy via randomized measurements, *Science* **364**, 260 (2019).
- [26] M. Tajik, I. Kukuljan, S. Sotiriadis, B. Rauer, T. Schweigler, F. Cataldini, J. Sabino, F. Møller, P. Schüttelkopf, S.-C. Ji, D. Sels, E. Demler, and J. Schmiedmayer, Verification of the area law of mutual information in a quantum field simulator, *Nat. Phys.* **19**, 1022 (2012).
- [27] T. Haas, Area laws from classical entropies, See same arXiv posting (2024).
- [28] U. Leonhardt and H. Paul, Measuring the quantum state of light, *Prog. Quantum. Electron.* **19**, 89 (1995).
- [29] G. Kirchmair, B. Vlastakis, Z. Leghtas, S. E. Nigg, H. Paik, E. Ginossar, M. Mirrahimi, L. Frunzio, S. M. Girvin, and R. J. Schoelkopf, Observation of quantum state collapse and revival due to the single-photon Kerr effect, *Nature* **495**, 205 (2013).
- [30] F. Haas, J. Volz, R. Gehr, J. Reichel, and J. Estève, Entangled states of more than 40 atoms in an optical

- fiber cavity, *Science* **344**, 180 (2014).
- [31] H. Strobel, W. Muessel, D. Linnemann, T. Zibold, D. B. Hume, L. Pezzè, A. Smerzi, and M. K. Oberthaler, Fisher information and entanglement of non-Gaussian spin states, *Science* **345**, 424 (2014).
- [32] G. Barontini, L. Hohmann, F. Haas, J. Estève, and J. Reichel, Deterministic generation of multiparticle entanglement by quantum Zeno dynamics, *Science* **349**, 1317 (2015).
- [33] C. Wang, Y. Y. Gao, P. Reinhold, R. W. Heeres, N. Ofek, K. Chou, C. Axline, M. Reagor, J. Blumoff, K. M. Sliwa, L. Frunzio, S. M. Girvin, L. Jiang, M. Mirrahimi, M. H. Devoret, and R. J. Schoelkopf, A Schrödinger cat living in two boxes, *Science* **352**, 1087 (2016).
- [34] P. Kunkel, M. Prüfer, H. Strobel, D. Linnemann, A. Frölian, T. Gasenzer, M. Gärtner, and M. K. Oberthaler, Spatially distributed multipartite entanglement enables EPR steering of atomic clouds, *Science* **360**, 413 (2018).
- [35] P. Kunkel, M. Prüfer, S. Lannig, R. Rosa-Medina, A. Bonnin, M. Gärtner, H. Strobel, and M. K. Oberthaler, Simultaneous Readout of Noncommuting Collective Spin Observables beyond the Standard Quantum Limit, *Phys. Rev. Lett.* **123**, 063603 (2019).
- [36] P. Kunkel, M. Prüfer, S. Lannig, R. Strohmaier, M. Gärtner, H. Strobel, and M. K. Oberthaler, Detecting Entanglement Structure in Continuous Many-Body Quantum Systems, *Phys. Rev. Lett.* **128**, 020402 (2022).
- [37] C. D. Hamley, C. S. Gerving, T. M. Hoang, E. M. Bookjans, and M. S. Chapman, Spin-nematic squeezed vacuum in a quantum gas, *Nat. Phys.* **8**, 305 (2012).
- [38] Y. Kawaguchi and M. Ueda, Spinor Bose-Einstein condensates, *Phys. Rep.* **520**, 253 (2012).
- [39] Y. Deller, M. Gärtner, T. Haas, M. K. Oberthaler, M. Reh, and H. Strobel, Area laws for classical entropies in a spin-1 Bose-Einstein condensate, Companion paper appearing in the same arXiv posting (2024).
- [40] See Supplemental Material at [URL will be inserted by publisher] for details.
- [41] A. Polkovnikov, Phase space representation of quantum dynamics, *Ann. Phys.* **325**, 1790 (2010).
- [42] P. Blakie, A. Bradley, M. Davis, R. Ballagh, and C. Gardiner, Dynamics and statistical mechanics of ultra-cold Bose gases using c-field techniques, *Adv. Phys.* **57**, 363 (2008).
- [43] C. Weedbrook, S. Pirandola, R. García-Patrón, N. J. Cerf, T. C. Ralph, J. H. Shapiro, and S. Lloyd, Gaussian quantum information, *Rev. Mod. Phys.* **84**, 621 (2012).
- [44] W. P. Schleich, *Quantum Optics in Phase Space* (Wiley-VCH Verlag Berlin, 2001).
- [45] L. Mandel and E. Wolf, *Optical Coherence and Quantum Optics* (Cambridge University Press, 2013).
- [46] P. Kunkel, *Splitting a Bose-Einstein condensate enables EPR steering and simultaneous readout of noncommuting observables*, Ph.D. thesis, Ruprecht-Karls-Universität Heidelberg (2019).
- [47] K. Husimi, Some formal properties of the density matrix, *Proc. Phys.-Math. Soc. Jap. 3rd Ser.* **22**, 264 (1940).
- [48] N. D. Cartwright, A non-negative Wigner-type distribution, *Phys. A* **83**, 210 (1976).
- [49] We have  $d\nu^A = d\phi^A d\pi^A$  for  $\mathcal{O}^A = \mathcal{W}^A$ ,  $d\nu^A = d\phi^A$  ( $d\nu^A = d\pi^A$ ) for  $\mathcal{O}^A = f^A$  ( $\mathcal{O}^A = g^A$ ) and  $d\nu^A = d\phi^A \pi^A / (2\pi)^{\dim A}$  for  $\mathcal{O}^A = \mathcal{Q}^A$ .
- [50] I. Białynicki-Birula and J. Mycielski, Uncertainty relations for information entropy in wave mechanics, *Commun. Math. Phys.* **44**, 129 (1975).
- [51] A. Wehrl, On the relation between classical and quantum-mechanical entropy, *Rep. Math. Phys.* **16**, 353 (1979).
- [52] E. H. Lieb, Proof of an entropy conjecture of Wehrl, *Commun. Math. Phys.* **62**, 35 (1978).
- [53] Z. Van Herstraeten and N. J. Cerf, Quantum Wigner entropy, *Phys. Rev. A* **104**, 042211 (2021).
- [54] S. Floerchinger, T. Haas, and H. Müller-Groeling, Wehrl entropy, entropic uncertainty relations, and entanglement, *Phys. Rev. A* **103**, 062222 (2021).
- [55] N. J. Cerf and T. Haas, Information and majorization theory for fermionic phase-space distributions, arXiv:2401.08523 (2024).
- [56] P. J. Coles, M. Berta, M. Tomamichel, and S. Wehner, Entropic uncertainty relations and their applications, *Rev. Mod. Phys.* **89**, 015002 (2017).
- [57] A. Hertz and N. J. Cerf, Continuous-variable entropic uncertainty relations, *J. Phys. A Math. Theor.* **52**, 173001 (2019).
- [58] S. Floerchinger, T. Haas, and M. Schröfl, Relative entropic uncertainty relation for scalar quantum fields, *SciPost Phys.* **12**, 089 (2022).
- [59] S. Ditsch and T. Haas, Entropic distinguishability of quantum fields in phase space, arXiv:2307.06128 (2023).
- [60] The proportionality constant is  $1 + \ln \pi$ ,  $(1 + \ln \pi)/2$  and 1 for the Wigner  $W$ , the marginal and the Husimi  $Q$ -distribution, respectively.
- [61] G. Adesso, D. Girolami, and A. Serafini, Measuring Gaussian Quantum Information and Correlations Using the Rényi Entropy of Order 2, *Phys. Rev. Lett.* **109**, 190502 (2012).
- [62] A. Serafini, *Quantum Continuous Variables* (CRC Press, 2017).
- [63] E. H. Lieb and R. Seiringer, Stronger subadditivity of entropy, *Phys. Rev. A* **71**, 062329 (2005).
- [64] The upper bound  $I(f^A : f^B) + I(g^A : g^B) \leq I(\rho^A : \rho^B)$  has been conjectured in [71].
- [65] M. M. Wolf, F. Verstraete, M. B. Hastings, and J. I. Cirac, Area laws in quantum systems: Mutual information and correlations, *Phys. Rev. Lett.* **100**, 070502 (2008).
- [66] L. F. Kozachenko and N. N. Leonenko, Sample Estimate of the Entropy of a Random Vector, *Probl. Peredachi Inf.* **23**, 9 (1987).
- [67] A. Kraskov, H. Stögbauer, and P. Grassberger, Estimating mutual information, *Phys. Rev. E* **69**, 066138 (2004).
- [68] G. V. Steeg, Non-parametric Entropy Estimation Toolbox, <https://github.com/gregversteeg/NPEET> (2014).
- [69] P. Pechukas, Reduced Dynamics Need Not Be Completely Positive, *Phys. Rev. Lett.* **73**, 1060 (1994).
- [70] J. S. Centre, JUWELS: Modular Tier-0/1 Supercomputer at the Jülich Supercomputing, JLSRF (2019).
- [71] J. Schneeloch, C. J. Broadbent, and J. C. Howell, Uncertainty relation for mutual information, *Phys. Rev. A* **90**, 062119 (2014).

## Supplementary material

### I. CLASSICAL WIGNER ENTROPY

We illustrate the extensive growth of standard classical entropies by plotting the full classical Wigner entropy, i.e. without subtracting the vacuum contribution, in [Figure 1](#).

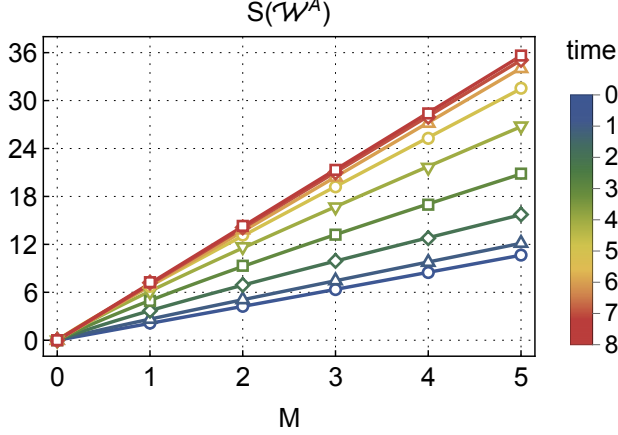


Figure 1. Time evolution of the full Wigner entropy  $S(\mathcal{W}^A)$  for which the leading-order volume law is apparent for all times. The area law is barely visible on top of the extensive growth in the early-time regime, i.e. for  $0 < t \leq 4$ . Note that at  $t = 0$  we have  $S(\mathcal{W}^A) = S(\tilde{\mathcal{W}}^A) = M(1 + \ln \pi) \approx 2.144M$ .

### II. NON-GAUSSIANITY

We consider a Gaussian model distribution

$$\mathcal{W}^{A,\text{Gauss}} = \frac{1}{Z^A} e^{-\frac{1}{2}(\chi^A)^T (\gamma^A)^{-1} \chi^A}, \quad (1)$$

where  $\chi^A = (\phi^A, \pi^A)^T$  is a vector in phase space,  $(\gamma^A)^{jj'} = \text{Tr}\{\rho^A\{\chi^j - \chi^j, \chi^{j'} - \chi^{j'}\}\}/2$  denotes the covariance matrix and  $Z^A = (2\pi)^M \sqrt{\det \gamma^A}$  is a normalization constant. To assess the non-Gaussianity of a given distribution  $\mathcal{W}^A$ , we introduce the Wigner relative entropy with respect to the nearest Gaussian, i.e. the distribution with the same first- and second-order moments [\[1, 2\]](#)

$$S(\mathcal{W}^A \parallel \mathcal{W}^{A,\text{Gauss}}) = \int d\nu^A \mathcal{W}^A \ln \frac{\mathcal{W}^A}{\mathcal{W}^{A,\text{Gauss}}}. \quad (2)$$

Then,  $\mathcal{W}^A$  is (non-)Gaussian if and only if  $S(\mathcal{W}^A \parallel \mathcal{W}^{A,\text{Gauss}})(>) = 0$ . The non-negativity of the Wigner relative entropy translates into a Gaussian upper bound on the subtracted Wigner entropy, i.e.  $\Delta S(\mathcal{W}^A) \leq \Delta S(\mathcal{W}^{A,\text{Gauss}})$ , showing that resolving non-Gaussian features decreases the missing information about the underlying distribution. In this sense,  $S(\mathcal{W}^A \parallel \mathcal{W}^{A,\text{Gauss}})$  measures the additional information encoded in  $\mathcal{W}^A$  with respect to  $\mathcal{W}^{A,\text{Gauss}}$ .

To calculate the Wigner relative entropy [\(2\)](#) without reconstructing any distribution, we use [\(1\)](#) and perform a few straightforward simplifications, leading to

$$S(\mathcal{W}^A \parallel \mathcal{W}^{A,\text{Gauss}}) = \Delta S(\mathcal{W}^{A,\text{Gauss}}) - \Delta S(\mathcal{W}^A). \quad (3)$$

While  $\Delta S(\mathcal{W}^A)$  is estimated using the  $k$ NN method, the subtracted Wigner entropy of the nearest Gaussian distribution is computed via

$$\Delta S(\mathcal{W}^{A,\text{Gauss}}) = \frac{1}{2} \ln \det (2\gamma^A), \quad (4)$$

such that only the covariance matrix has to be extracted from the TWA samples. We show the resulting relative entropy curves in [Figure 2](#) for all times discussed in the main text.

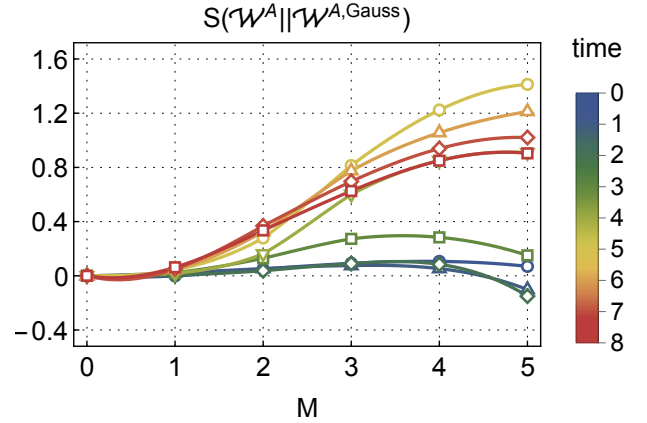


Figure 2. Time evolution of the non-Gaussianity measure  $S(\mathcal{W}^A \parallel \mathcal{W}^{A,\text{Gauss}})$ . Single-well distributions look rather Gaussian, while non-Gaussian features become apparent for larger subsystems. The non-Gaussianity is negligible for early times and peaks around  $t \approx 5$ , for which the relative information difference is  $\sim 8\%$ . We checked negative values at  $M = 5$  for early times are caused by an insufficient number of samples, see [\[3\]](#) for details.

### III. MODE OCCUPATIONS FOR LATE TIMES

*A priori*, it is unclear whether TWA gives meaningful results in the late-time limit where local thermalization occurs. As a semi-classical approximation, TWA is expected to hold whenever the momentum modes are occupied mesoscopically, that is, filled up to at least roughly one order of magnitude above the quantum one-half [\[4–7\]](#). In [Figure 3](#), we confirm that this condition is fulfilled for late times by plotting the momentum-mode occupations  $n_{m_F}(k) = \langle \mathbf{a}_{m_F}^{k\dagger} \mathbf{a}_{m_F}^k \rangle$  for the zero mode (left panel), the side modes (middle panel) and their sum (right panel).

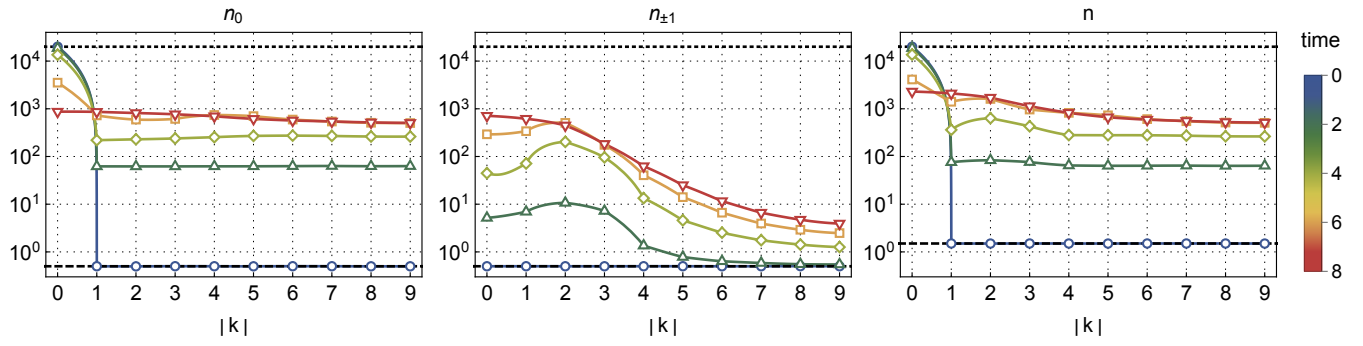


Figure 3. Dynamics of the momentum-mode occupations for the zero mode (left), the side modes (middle) and their sum (right). The atom number  $n = 2 \times 10^4$  and the quantum one-half (three-half) are depicted by dotted and dashed lines, respectively.

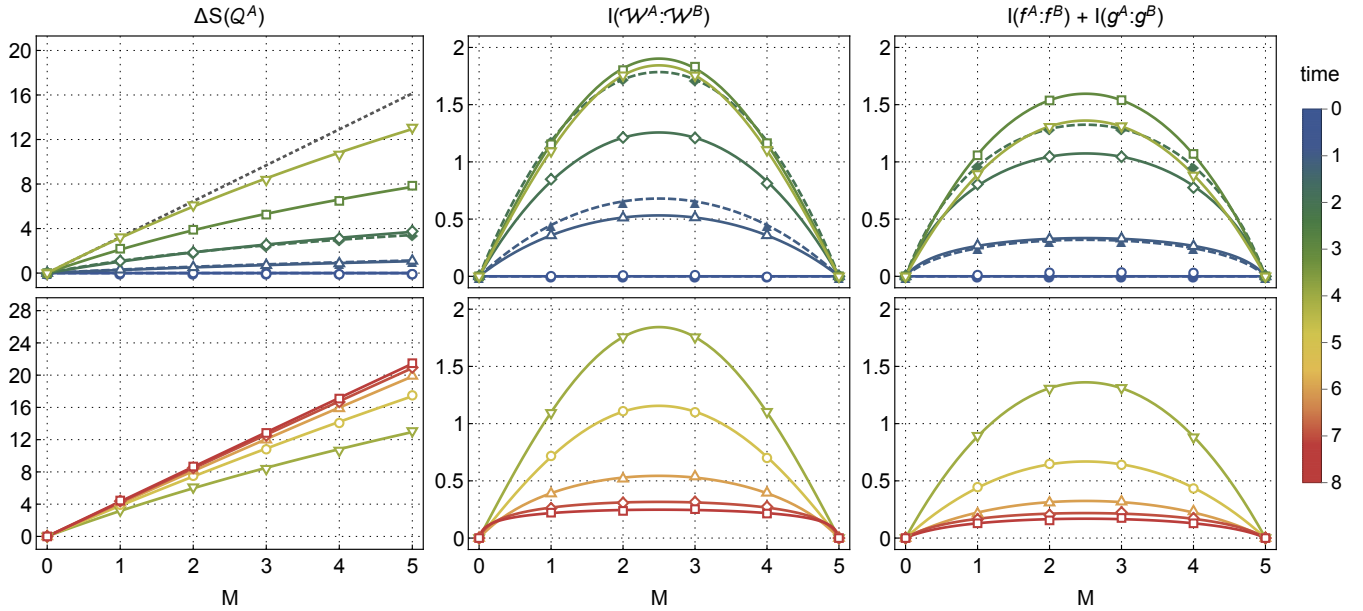


Figure 4. Same analysis as in Fig. 2 in the main text for the subtracted Wehrl entropy (left column), the Wigner mutual information (middle column) and the marginal mutual information sum (right column). All observed quantum features carry over to these three quantities as well. The local temperature  $T \approx 5$  is also observed for the subtracted Wehrl entropy. Note here that the latter is based on the differently normalized Husimi  $Q$ -distribution, which we accounted for by subtracting  $M \ln 2$ .

#### IV. OTHER CLASSICAL INFORMATION-THEORETIC MEASURES

In analogy to Figure 2 in the main text, we show the dynamics of the subtracted Wehrl entropy  $\Delta S(Q^A)$ ,

the Wigner mutual information  $I(\mathcal{W}^A : \mathcal{W}^B)$  and the marginal mutual information sum  $I(f^A : f^B) + I(g^A : g^B)$  in Figure 4. All quantities behave as expected.

- 
- [1] S. Floerchinger, T. Haas, and M. Schröfl, Relative entropic uncertainty relation for scalar quantum fields, *SciPost Phys.* **12**, 089 (2022).
- [2] S. Ditsch and T. Haas, Entropic distinguishability of quantum fields in phase space, [arXiv:2307.06128](https://arxiv.org/abs/2307.06128) (2023).
- [3] Y. Deller, M. Gärtner, T. Haas, M. K. Oberthaler, M. Reh, and H. Strobel, Area laws for classical entropies in a spin-1 Bose-Einstein condensate, Companion paper appearing in the same arXiv posting (2024).
- [4] M. Werner and P. Drummond, Robust Algorithms for Solving Stochastic Partial Differential Equations, *J. Comp. Phys.* **132**, 312–326 (1997).
- [5] M. J. Steel, M. K. Olsen, L. I. Plimak, P. D. Drummond, S. M. Tan, M. J. Collett, D. F. Walls, and R. Graham, Dynamical quantum noise in trapped Bose-Einstein condensates, *Phys. Rev. A* **58**, 4824–4835 (1998).

- [6] A. Sinatra, C. Lobo, and Y. Castin, Classical-Field Method for Time Dependent Bose-Einstein Condensed Gases, *Phys. Rev. Lett.* **87**, 210404 (2001).
- [7] A. Sinatra, C. Lobo, and Y. Castin, The truncated Wigner method for Bose-condensed gases: limits of validity and applications, *J. Phys. B: At. Mol. Opt. Phys.* **35**, 3599–3631 (2002).